IOPscience iopscience.iop.org

Home Search Collections Journals About Contact us My IOPscience

Topochemical reactions of layered transition-metal oxides

This content has been downloaded from IOPscience. Please scroll down to see the full text.

2014 Semicond. Sci. Technol. 29 064010

(http://iopscience.iop.org/0268-1242/29/6/064010)

View the table of contents for this issue, or go to the journal homepage for more

Download details:

IP Address: 129.120.87.225
This content was downloaded on 07/02/2017 at 17:17

Please note that terms and conditions apply.

You may also be interested in:

Cathode materials based on perovskite-like transition metal oxides for intermediate temperature solid oxide fuel cells
S Ya Istomin and E V Antipov

High-temperature superconductors based on complex layered copper oxyfluorides
Artem M Abakumov, Marina G Rozova, Elena I Ardashnikova et al.

Transport and other physical properties of perovskites
J B Goodenough

PbY1xCaxBa2Cu3O7F2: synthesis, structure and superconductivity
A L Kirbyshire and C Greaves

Recent research progress on iron- and manganese-based positive electrode materials for rechargeable sodium batteries
Naoaki Yabuuchi and Shinichi Komaba

Solid State Ionics: from Michael Faraday to green energy—the European dimension
Klaus Funke

Complex manganese oxides with the brownmillerite structure: synthesis, crystal chemistry and properties
Artem M Abakumov, Marina G Rozova and Evgenii V Antipov

Crystal structures and conduction processes
Stephen Hull

IOP Publishing Semiconductor Science and Technology
Semicond. Sci. Technol. 29 (2014) 064010 (8pp) doi:10.1088/0268-1242/29/6/064010

Topochemical reactions of layered transition-metal oxides

M A Hayward

Department of Chemistry, University of Oxford, Inorganic Chemistry Laboratory, South Parks Road, Oxford, OX1 3QR, UK

E-mail: michael.hayward@chem.ox.ac.uk

Received 19 November 2013, revised 16 December 2013
Accepted for publication 19 December 2013
Published 6 May 2014

Abstract

Low-temperature topochemical reactions performed on complex transition metal oxides allow the synthesis of novel, metastable phases often with unusual transition metal oxidation states and/or coordination geometries. Layered materials offer many opportunities to control the structural and chemical selectivity of these types of reactions to allow the preparation of desired phases in a rational manner. Using complex oxides adopting Ruddlesden–Popper type structures as examples, recent progress in the low-temperature topochemical reduction by anion de-intercalation, and oxidation by anion insertion, is reviewed.

Keywords: topochemical reduction, topochemical oxidation, transition metal oxide

(Some figures may appear in colour only in the online journal)

Introduction

The synthesis of complex metal oxides is typically achieved via 'ceramic' reactions in which mixtures of binary metal oxides or oxo-acids are reacted at high temperature (T > 900 °C). These elevated synthesis temperatures are required because there are large energetic barriers opposing the diffusion of species in the solid state. These barriers to diffusion are generally so large that mass transport makes a dominant contribution to the activation energy of reactions between solid reagents. Given that the motion and diffusion of chemical species is a common feature of all solid–solid reactions, it follows that the activation energies of competing solid–solid reactions tend to be comparable. Thus, at the high temperatures required to overcome these large activation energies, the products of a large number of competing reactions are energetically accessible and in equilibrium with each other, resulting in the formation of the most thermodynamically stable phase or mixture of phases. As a result, high-temperature synthesis routes operate under 'thermodynamic control' and are restricted to forming only the most thermodynamically stable phase or mixture of phases for a given composition, precluding the formation of a large number of metastable materials.

In contrast to ceramic reactions, low-temperature topochemical reaction schemes seek to prepare metastable phases by exerting some 'kinetic' control over the selection of product phases. Under kinetic control the product is the phase which forms fastest rather than the phase which is most thermodynamically stable. Kinetic control can be exerted in solid state reactions by utilizing the different rates of solid-state diffusion of different species, as these correspond to differences in reactivity. For example, in many complex oxides one class of ions, be it a cation (e.g. Li^+, Na^+ etc) or an anion (O^{2-}, F^- etc), is often considerably more mobile at a given temperature than the surrounding host lattice. As a consequence, these mobile species can be inserted into, or removed from, host phases at low temperature, under conditions in which the surrounding lattice is effectively immobile, to yield metastable phases which are generally inaccessible by high-temperature synthesis routes. Chemical transformations of this type are described as 'topochemical' because, unlike the majority of high-temperature reactions, they conserve the basic structural topology of the host material. This retention of structure between reactants and products allows a degree of synthesis planning and product targeting which is generally unavailable in high-temperature syntheses.

Layered complex oxide phases offer many opportunities for the preparation of new metastable materials by topochemical reaction routes. Layered materials naturally exhibit anisotropic bonding interactions which can amplify the mobility differences between species. In addition, the

 © 2014 IOP Publishing Ltd Printed in the UK

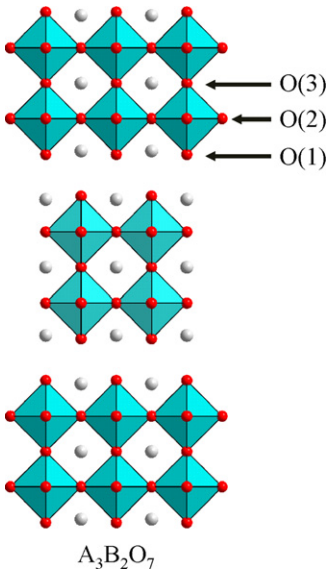

Figure 1. The topologically distinct anions sites in the $n = 2$ Ruddlesden–Popper structure.

layered topology of materials tends to result in phases which contain cations or anions in a number of topologically distinct coordination sites, allowing a degree of selectivity to be imposed on topochemical reactions. Focusing on the low-temperature anion chemistry of complex layered oxides and using materials adopting Ruddlesden–Popper-type structures as examples [1], this review seeks to highlight some of the opportunities low-temperature topochemical reactions present to prepare new phases, or modify existing materials, in a rational manner.

Selectivity of anion deintercalation reactions of layered oxide phases

Topochemical reduction reactions seek to deintercalate anions from extended solids at low temperature to yield reduced materials, which cannot be prepared via high-temperature ceramic routes, containing metal centres in unusual oxidation states and/or coordination geometries. Typically reactions of this type are performed using hydrogen gas, metal getters or binary metal hydrides as reducing agents, and the relative merits of these different approaches have been discussed in a number of recent reviews [2–5]. Here we consider a different aspect of topochemical reduction reactions: structural selectivity. Which anions are removed during the reduction process? Can this be controlled to yield anion deficient materials with desired vacancy ordering patterns?

As noted above, complex oxide phases with layered structures naturally contain a number of different 'topologically distinct' anion sites. For example, the $n = 2$ Ruddlesden–Popper structure [1] shown in figure 1, has three topologically distinct anion sites: O(1) the apical site adjacent to the rocksalt layer, O(2) the equatorial site and O(3) the apical site in the perovskite block. We can describe these different anion sites as topologically distinct, rather than simply crystallographically distinct, because they are situated at different positions within the structural network and cannot be made equivalent by simply removing a symmetry-breaking tilting or twisting distortion. As a counter example, the two crystallographically distinct oxide ion sites in a $GdFeO_3$-type distorted perovskite structure are not topologically distinct because they can be made equivalent by removing the cooperative twisting distortion.

Anions situated in topologically distinct coordination sites tend to exist in different chemical environments, for example in $A_3B_2O_7$, $n = 2$ Ruddlesden–Popper phases the O(1) site resides in an A_5B coordination site compared to the A_4B_2 coordination of the O(2) and O(3) sites, and as a result anions in different topochemically distinct sites are likely to have different mobilities. In addition, and generally of greater importance, the removal of anions from different topologically distinct sites will have different consequences for the stability (lattice energy) of the resulting topochemically reduced phases. These differences, if understood, could in principal be used to predict the structural selectivity of topochemical reduction reactions so that by the careful selection or modification of host phases, anion deficient materials with desired anion-vacancy ordering schemes can be prepared via low-temperature reduction reactions.

The topochemical reduction reactions of a number of $A_3B_2O_7$, $n = 2$ Ruddlesden–Popper phases containing late 3d transition metals (Mn, Fe, Co, Ni) have been studied and these materials provide a good set of example phases to illustrate the factors which direct the selectivity of oxygen deintercalation reactions.

Manganese containing anion deficient $A_3Mn_2O_{7-\delta}$ Ruddlesden–Popper phases are observed to exhibit structures in which the induced anion vacancies are located on either the O(2) or O(3) anion sites. For example the anion deficient phase $Sr_3Mn_2O_{6+\delta}$ [6], prepared at high temperature and thus under thermodynamic control, contains anion vacancies that reside exclusively in the O(2) equatorial anion sites of the phase, indicating a thermodynamic preference for locating anion vacancies on this site, in this system. However, if we consider the mixed valent $Mn^{3+/4+}$ phases of composition $RESr_2Mn_2O_7$ (RE = Y, Lanthanide), we observe the anion deficient phases prepared by the reduction of $NdSr_2Mn_2O_7$ contain anion vacancies located on the O(3) anion site [7], while the topochemical reduction of the isoelectronic phase $YSr_2Mn_2O_7$ results in $YSr_2Mn_2O_{5.5}$, a phase in which all the anion vacancies are located on the O(2) anion site [8].

All three of the examples exhibit a strong structural preference for locating anion vacancies in either the O(2) or O(3) sites, but not both. When this is combined with the observation that the reductions of $Sr_3Mn_2O_7$ and $NdSr_2Mn_2O_7$ occur at high temperature, this suggests that the observed selectivity is being driven by thermodynamic considerations (the stability of the anion deficient phases) rather than kinetic considerations (the different mobilities of the topologically distinct anion sites).

While it is clearly possible to perform detailed calculations to determine the relative stabilities of different anion-vacancy arrangements within the $n = 2$ Ruddlesden–Popper structural framework, this can be computationally

Table 1. The calculated anion bond valence sums from some $A_3B_2O_7$ $n = 2$ Ruddlesden–Popper phases.

Anion	Anion BVS	$Sr_3Mn_2O_7$	$YSr_2Mn_2O_7$	$NdSr_2Mn_2O_7$	$La_3Ni_2O_7$	$Sr_3Fe_2O_7$	$Sr_3Fe_2O_5Cl_2$	$Sr_3Co_2O_5Cl_2$
O(1)	BVS A	1.197	1.227	1.181	1.127	1.126	1.155	1.184
	BVS B	0.661	0.473	0.508	0.302	0.619	0.086	0.059
	(BVS B) − (BVS A)	−0.536	−0.0754	−0.601	−0.824	−0.504	−1.069	−1.125
O(2)	BVS A	0.960	0.914	0.940	1.095	0.912	0.871	0.874
	BVS B	1.344	1.311	1.263	0.966	1.270	1.068	0.923
	(BVS B) − (BVS A)	**+0.384**	**+0.397**	+0.322	**−0.129**	+0.358	+0.197	+0.047
O(3)	BVS A	0.856	0.978	0.779	0.839	0.776	0.649	0.692
	BVS B	1.170	1.146	1.253	1.000	1.168	1.474	1.219
	(BVS B) − (BVS A)	+0.314	+0.168	**+0.473**	−0.160	**+0.392**	**+0.825**	**+0.529**

expensive and is likely to be beyond the technical capabilities of many researchers who are not primarily focused on theory. To try to fill this gap we have developed a crude, 'rough and ready' method involving the analysis of anion bond valence sums (BVS), which allows us to explain the observed structural selectivities of anion deintercalation reactions (within the caveats and constraints detailed below) and to make general predictions about the likely outcome of topochemical reduction reactions of as yet unstudied systems.

The strategy for deducing which of the different topologically distinct anion sites can host anion vacancies with the smallest thermodynamic 'cost' is based on a number of assumptions:

(i) The anions in all the topologically distinct anion sites are 'mobile' and the topochemically reduced phase formed will adopt a structure with the lowest energy, within the constraint that the topology of the cation lattice must be conserved.
(ii) The oxygen stoichiometric host phase is at a thermodynamic minimum (i.e. it is the most stable configuration that can be formed with that composition).
(iii) The free energy of the topochemically reduced product phase can be considered as a small perturbation of the free energy of the host phase, and it is the size of this perturbation which is important, not the absolute stability of the reduced phase.
(iv) None of the metal cations in the system has an energetically 'preferred' coordination geometry—as noted below this is the assumption that is most commonly observed to be incorrect.

The approach we have taken is to consider the optimal changes to the local metal coordination polyhedra on reduction which would stabilize the reduced product. If we consider the BVS of the B-cations [9], this clearly needs to decline on oxygen deintercalation due to the reduction of the transition metal B-cations, thus the B-cation coordination number should decline and/or the average B–O bond length increase. In contrast, the oxidation state of the A-cations is unchanged on oxygen deintercalation, so the BVS of these cations needs to be maintained, favouring a minimal change to the local A-cation coordination environment. The best compromise between the two largely incompatible requirements of the two cation classes, is to remove oxide ions with short (strong) bonds to the B-cations and weak (long) bonds to the A-cations, as this will lead to a largest decline in the B-cation BVS for the smallest change in the A-cation BVS. We can evaluate this idea by calculating the contribution each anion site makes to the BVS of the A- and B-cations (table 1), with our expectation being that the anions removed on reduction are those with the largest value of (BVS B)–(BVS A). It should be noted that in this instance BVS are not being used to calculate the 'valence' of the cations in the structure, they are instead being used to crudely compare the contribution each cation–anion contact makes to the lattice energy of the phase, without calculating it explicitly.

As shown in table 1 this method works well for manganese containing $n = 2$ Ruddlesden–Popper phases, indicating that anions will be removed from the O(2) sites of $Sr_3Mn_2O_7$ and $YSr_2Mn_2O_7$ and the O(3) sites of $NdSr_2Mn_2O_7$, in agreement with experimental observations [6–8]. Analogous analyses have also correctly identified the site from which anions are removed during topochemical reduction for a number of other manganese containing phases such as $Sr_4Mn_3O_{7.5}Cl_2$ and $Sr_7Mn_4O_{15}$ [10–12], suggesting that if the assumptions stated above hold, this is a useful method for predicting from which topologically distinct site anions will be removed on reduction, in a wide variety of materials.

The reduction reactions of $NdSr_2Mn_2O_7$ and $YSr_2Mn_2O_7$, described above, exhibit differing structural selectivities, despite being isoelectronic and essentially isostructural [7, 8]. This suggests that the identity of the A-cations can be used to direct the progress and structural selectivity of anion deintercalation reactions in some host lattices. Similar behaviour has also been observed during the topochemical reduction of layered $REBaCo_2O_5$ (RE = Y, lanthanide) cation-ordered perovskite phases, in which the reduction of $YBaCo_2O_5$ and $LaBaCo_2O_5$ yield topochemically reduced products with distinctly different anion-vacancy distributions (the latter, $LaBaCo_2O_{4.25}$ containing square-planar Co^{1+} centres), despite the two host phases being isoelectronic and isostructural [13].

Another general feature which comes out of the bond valence sum analysis is that, as shown in table 1, the O(1) apical site consistently has the most negative, unfavourable value of (BVS B)–(BVS A). This is attributable to the A_5B coordination of this anion site, compared to the A_4B_2 coordination of the other anion sites, and leads to the general expectation that anions will not be removed during topochemical reactions from the O(1) sites of phases with this structure type. This

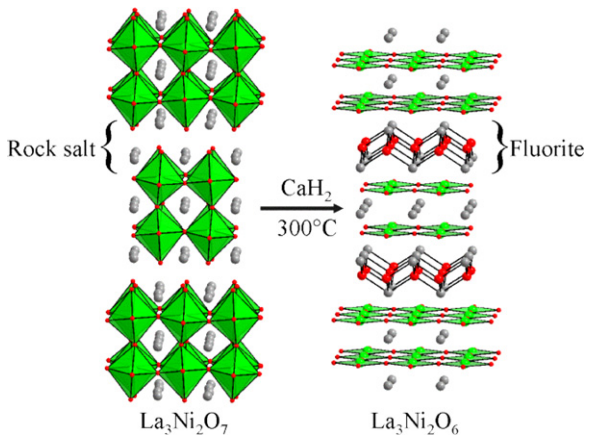

Figure 2. Topochemical reduction of $La_3Ni_2O_7$ occurs in association with a rearrangement of the anion lattice to yield $La_3N_2O_6$, a phase containing square-planar NiO_4 units.

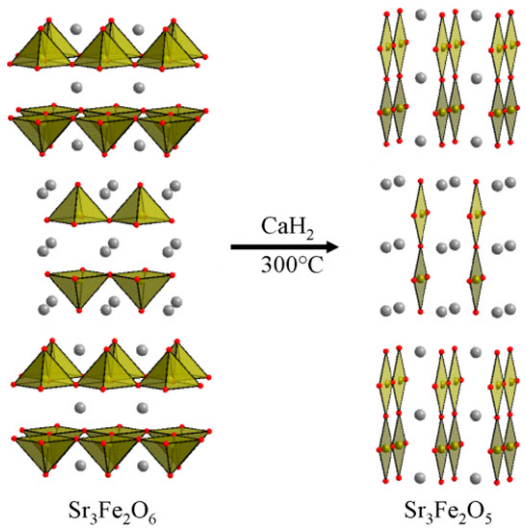

Figure 3. Topochemical reduction of $Sr_3Fe_2O_6$ yields $Sr_3Fe_2O_5$, a phase containing square-planar $Fe(II)O_4$ units.

general rule can be extended to phases with other Ruddlesden–Popper and related structures and is borne out by observing that during the topochemical reduction of $n = 1$ Ruddlesden–Popper phases of the form A_2MO_4 (M = Mn, Fe, Ru, Co, Ni) [14–20], oxide ions are deintercalated exclusively from the equatorial anion sites, not the axial anion sites analogous to the O(1) site in the $n = 2$ Ruddlesden–Popper structure.

As noted above the 'bond valence sum prediction method' makes the assumption that the transition metal cations have no electronically preferred geometry or connectivity and that topochemical reduction reactions proceed via the simple deintercalation of oxide ions. In many cases however these assumptions are not valid. For example, reduction of $La_3Ni_2O_7$ is predicted to occur via the deintercalation of oxide ions from the O(2) equatorial anion site (table 1), however reaction of $La_3Ni_2O_7$ with CaH_2 forms $La_3Ni_2O_6$ which adopts a structure related to the T'-structure of Nd_2CuO_4, as shown in figure 2 [21]. During the reduction of $La_3Ni_2O_7$ the apical O(1) oxide ions which reside within rock salt layers of the host phase migrate into coordination sites analogous to those adopted by fluoride ions in the fluorite structure, while oxide ions are simultaneously deintercalated from the O(3) anion site. As a result the nickel cations in the reduced product are located within apex-linked NiO_4 square planes (figure 2), a configuration which is stabilized by the $d^{8/9}$ electronic configuration of the $Ni^{2+/1+}$ cations.

The reduction reactions of iron containing phases also appear to show a coordination geometry preference. The initial reduction of $Sr_3Fe_2O_{7-\delta}$ to $Sr_3Fe_2O_6$ proceeds via the deintercalation of oxide anions from the O(3) anion site, as predicted in table 1 [22], however further reduction to form the Fe(II) phase $Sr_3Fe_2O_5$ proceeds not via the further simple removal of anions from the O(2) anion site, but instead via a reorganisation of the anion lattice to form a highly unusual array of apex-linked, square-planar $Fe(II)O_4$ units, in a process which 'refills' the O(3) anion site, as shown in figure 3 [23]. This anion lattice rearrangement is consistent with the Fe(II) centres in the reduced product 'preferring' a square-planar geometry. It is hard to rationalize the preference of d^6 Fe^{2+} centres to adopt square-planar coordination geometries on electronic grounds, however a similar preference is observed during the reduction of the perovskite $SrFeO_{3-\delta}$ to the infinite layer phase $SrFeO_2$ [24, 25]. In this latter case, partial substitution of >30% cobalt or manganese for iron in the starting phase, changes the structure of the reduced product [26], while substitution of 50% ruthenium does not [27], supporting the idea that a d^6 electronic configuration of the Fe^{2+} cations (or substituted Ru^{2+} cations) drives the formation of product phases with square-planar coordination sites.

By using a combination of BVS predication and an appreciation of the preferred geometry of particular transition metal cations, host phases can be selected to favour the formation of desired metal–oxygen frameworks in the materials formed on subsequent reduction. For example, reduction of iron containing phase in the $Sr_{n+1}Fe_nO_{3n+1}$ ($n = 1, 2, \infty$) series yields Sr_2FeO_3, $Sr_3Fe_2O_5$ and $SrFeO_2$ [17, 23, 24].

All three Fe(II) phases have structures constructed from apex-linked, square-planar FeO_4 units. In the structures of Sr_2FeO_3 and $Sr_3Fe_2O_5$ these units are arranged as one-dimensional chains, or double chains, while in the structure of $SrFeO_2$ the FeO_4 squares are connected into infinite sheets which are stacked to form an essentially three-dimensional structure. However, there is no two-dimensional material formed containing planar FeO_4 units. A two-dimensional phase can be 'designed' by observing that the oxychloride structural analogue of $Sr_3Fe_2O_7$, $Sr_3Fe_2O_5Cl_2$, has sufficiently long Fe–Cl bonds (2.99 Å) that the Fe(III) centres can be considered 5-coordinate (figure 4) [28]. In addition bond valence analysis (table 1) suggests that the reduction of $Sr_3Fe_2O_5Cl_2$ should proceed via the removal of oxide ions from the O(3) anion site, to yield a material consisting of square-planar FeO_4 centres arranged in pairs of infinite sheets, separated by SrCl rocksalt spacing layers. Reaction of $Sr_3Fe_2O_5Cl_2$ with LiH leads to the formation of $Sr_3Fe_2O_4Cl_2$, which as predicted adopts a two-dimensional structure (figure 4) [29]. Furthermore because the formation of the

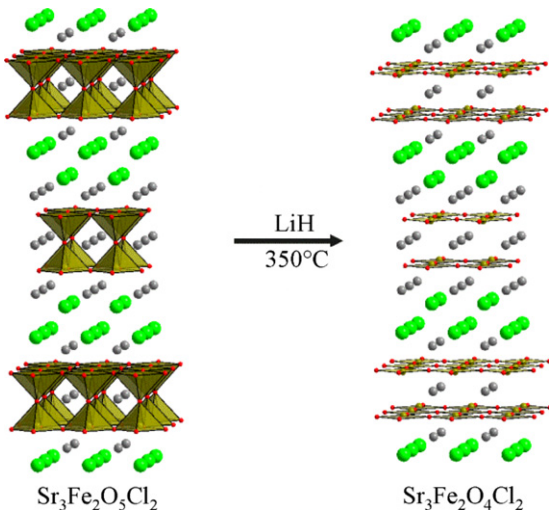

Figure 4. Topochemical reduction of $Sr_3Fe_2O_5Cl_2$ yields $Sr_3Fe_2O_4Cl_2$, containing infinite sheets of apex-linked Fe(II)O_4 units.

$A_3M_2O_4Cl_2$ framework is guided in part by the arrangement of the $A_3M_2O_5Cl_2$ lattice, and not just the coordination preferences of the M-cations, it is possible to substitute iron with cobalt and form isostructural phases across the whole $Sr_3Fe_{2-x}Co_xO_4Cl_2$ ($0 < x < 2$) composition range, via the reduction of the appropriate $Sr_3Fe_{2-x}Co_xO_5Cl_2$ host [30, 31]—an option not available in the materials based on the reduction of $Sr_{n+1}Fe_nO_{3n+1}$ hosts where the structure of reduced products is principally directed by the transition metal electron count.

The ability to make cation substitutions without inducing changes to the structure of the reduced products, allows the physical behaviour of materials with this unusual metal–oxygen frameworks to be studied as a function of electron count. In this instance $Sr_3Fe_2O_4Cl_2$ adopts and antiferromagnetically ordered state at high temperature ($T_N =$ 378 K) in common with the related $Sr_{n+1}Fe_nO_{2n+1}$ phases [29]. Partial substitution of iron with cobalt suppresses antiferromagnetic order, with spin-glass behaviour observed at $x \sim 1$ [30]. On complete replacement of all the iron with cobalt, antiferromagnetic order is recovered, although with a much lower ordering temperature ($T_N = 50$ K) and an inversion of the sign of the interlayer coupling [31]. Another consequence of replacing d^6 Fe^{2+} centres with d^7 Co^{2+} centres is that the local electronic configuration of the transition metal cations changes from $(d_z^2)^2$ $(d_{xz}, d_{yz})^2$ $(d_{xy})^1$ $(d_{x^2-y^2})^1$ to $(d_z^2)^2$ $(d_{xz}, d_{yz})^3$ $(d_{xy})^1$ $(d_{x^2-y^2})^1$. Thus, the local electronic configuration of cobalt centres in $Sr_3Co_2O_4Cl_2$ is orbitally degenerate and unstable with respect to a Jahn–Teller-like distortion which lifts this degeneracy. This manifests itself as a change from tetragonal ($I4/mmm$) to orthorhombic ($Immm$) crystal symmetry at $T \sim 200$ K.

Thus, by understanding the factors influencing the selectivity of topochemical reduction reactions, suitable starting materials can be selected to favour the formation of desired anion-deficient materials in a rational manner.

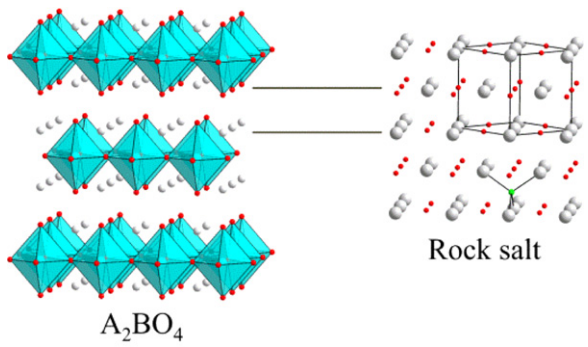

Figure 5. The rock salt layers in Ruddlesden–Popper phases contain 'tetrahedral' interstitial sites into which additional anions can be inserted.

Anion insertion into Ruddlesden–Popper oxide phases

In addition to directing the progress of anion deintercalation reactions, the anisotropic bonding patterns present in layered phases also allow species be topochemically inserted into materials. As the bonding schemes in layered materials tend to organize themselves such that interlayer bonding forces are much weaker than intralayer interactions, additional species (ions, small molecules, or molecular ions) can often be inserted between weakly bound layers, driving changes to the electronic behaviour and structures of materials.

While it may appear at first sight that Ruddlesden–Popper phases are dense and thus have no suitable coordination sites for the incorporation of additional species, the anisotropic nature of these structures means that there are interstitial sites in their frameworks which can be expanded to accommodate additional anions. As shown in figure 5, the $AO(ABO_3)_n$ Ruddlesden–Popper family of phases is constructed from 'perovskite' blocks n layers thick, separated by AO rocksalt layers. The A-cations within these rocksalt layers are arranged in a manner analogous to the cubic close-packed (CCP) arrangement of cations in the rocksalt structure, with oxide ions located in the 'octahedral' interstitial sites, again in an analogy to the rocksalt structure. As a result, the 'tetrahedral' interstitial sites present in the CCP array of A-cations are vacant and can accommodate additional anions inserted via topochemical processes, if the lattice expands appropriately. By this route La_2MO_4 (M = Co, Ni, Cu) $n = 1$ Ruddlesden–Popper phases can be oxidized either by heating at low temperature under oxygen pressure, or electrochemically in a KOH electrolyte [32–36].

Crystallographic studies have shown that the oxidation proceeds via the topochemical intercalation of oxide ions into the tetrahedral anion sites within the rocksalt layers of these phases to yield materials of composition $La_2MO_{4+\delta}$ ($0 \leqslant 0.15$). The insertion of oxygen into La_2MO_4 phases leads to a mild oxidation of the M^{2+} cations, which in the case of La_2CuO_4 drives a change from semiconducting to metallic behaviour, with superconductivity observed a low temperature with suitable levels of oxidation [34].

An unusual feature of the topochemical oxidation reactions of these Ruddlesden–Popper phases is that the anions

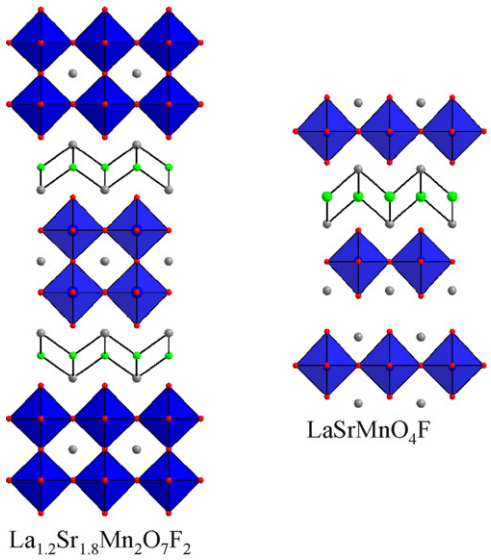

Figure 6. The structures of $La_{1.2}Sr_{1.8}Mn_2O_7F_2$ and $LaSrMnO_4F$.

are inserted into locations within the host phase which are not within the coordination spheres of the transition metal cations being oxidized. As a result, the oxidation state of the transition metal is changed (raised) while the local coordination at that transition metal site, and thus the d-orbital energies of the metal centre, remain largely unchanged. Modification of the electron count in this independent, isolated manner is much more typical of cation insertion or substitution than manipulation of the anion lattice, which tends to insert or remove anions from within the coordination spheres of the redox active transition metal centres, as observed for the anion deintercalations described above. Therefore, these 'remote' anion insertions into rock salt layers of Ruddlesden–Popper phases can be thought of as almost pure electronic doping processes.

In addition to 'hole doping' the host phase, the addition of low concentrations of interstitial oxide anions into $n = 1$ Ruddlesden–Popper phases allows these materials to exhibit reasonable oxide ion conductivity. Thus $La_2NiO_{4.15}$ is proposed as a cathode material for incorporation into solid oxide fuel cells [37–39]. Building on this idea, phases with larger concentrations of inserted anions have been sought, leading to the recent discovery of $La_{1.2}Sr_{0.8}MnO_{4.42}$ prepared via the oxidation of the $n = 1$ Ruddlesden–Popper phase $La_{1.2}Sr_{0.8}MnO_4$ [40].

In addition to the insertion of oxide ions, extensive investigations have revealed that through soft fluorination chemistry, fluoride ions can also be intercalated into the rock salt layers of Ruddlesden–Popper phases. For example reaction of the mixed valent $Mn^{3+/4+}$ $n = 2$ Ruddlesden–Popper phase $Ln_{1.2}Sr_{1.8}Mn_2O_7$ (Ln = La, Pr, Nd, Sm, Eu, Gd) with dilute fluorine gas or poly(vinylidene fluoride) yields $Ln_{1.2}Sr_{1.8}Mn_2O_7F_2$ [41, 42] a material in which fluoride ions have been inserted into the 'tetrahedral' interstitial sites of the A-cation sheet adopting an arrangement reminiscent of the CaF_2 fluorite structure (figure 6).

Analogous reactions performed on the $n = 1$ Ruddlesden–Popper phase $LaSrMnO_4$ lead to the formation of $LaSrMnO_4F_{1.7}$ in which the 'tetrahedral' interstitial sites are only partially filled [41]. The level of intercalation appears to be limited in this case by the ability to stabilize high manganese oxidation states. If $LaSrMnO_4F_{1.7}$ is heated with the appropriate amount of $LaSrMnO_4$, the Mn(IV) phase $LaSrMnO_4F$ can be formed via the thermal equilibration of the fluorine concentration. The resulting oxy-fluoride phase adopts a novel staged structure in which the anion intercalation sites in adjacent layers alternate between full and empty (figure 6) [43]. This staging behaviour suggests there is a large energy penalty associated with expanding the rock salt layers to make them suitable for anion intercalation and that this 'penalty' is only worth paying if all the anion intercalation sites within a layer are filled, in a situation strongly reminiscent of some cation intercalation reactions of layered host phases.

It should be noted that these fluorination reactions must be performed with the rigorous exclusion of water to prevent the formation of large quantities of binary metal fluoride impurities such as SrF_2. In an attempt to simplify the often elaborate experimental set ups required to handle and perform reactions with fluorine whilst rigorously excluding water, a number of other fluorinating strategies have been investigated. For example binary metal fluorides of late transition metals (MF_2, M = Ni, Cu, Zn, Ag) have been used to fluorinate Ruddlesden–Popper phases [44]. Heating a 1:1 mixture of the $n = 2$ Ruddlesden–Popper phase $Sr_3Ru_2O_7$ with CuF_2 in air at temperatures up to 300 °C yields the Ru(V) phase $Sr_3Ru_2O_7F_2$ and CuO [45]. It appears that the metal fluorides act as an *in situ* source of fluorine through reaction with oxygen according to reaction scheme (1) [46], and that this fluorine then rapidly reacts with the host phase to give the overall reaction (2)

$$MF_2 + {}^1\!/_2O_2 \rightarrow MO + \text{'}F_2\text{'} \quad (1)$$

$$Sr_3Ru_2O_7 + CuF_2 + {}^1\!/_2O_2 \rightarrow Sr_3Ru_2O_7F_2 + CuO. \quad (2)$$

It can be seen from these reaction schemes that the oxygen gas is acting as the oxidant and the metal fluoride only acts as a fluorine source. The use of metal fluorides as fluorinating agents not only eases the practical difficulties associated with handling fluorine, it is also observed to produce lower levels of binary fluoride impurities than reaction with elemental fluorine, presumably due to the rigorous exclusion of water. It should be noted however, that samples fluorinated in this manner almost inevitably become contaminated with the binary oxide by-products of the reaction, which are often hard to separate. It is possible in some cases to perform the fluorination reactions with the metal fluoride and host phase physically separated. If CuF_2 is heated at 500 °C under flowing oxygen, such that reaction (1) occurs and then the resulting mixture of gases are passed over the phase to be fluorinated, materials can in some cases be fluorinated without contamination by binary oxides [47].

The oxidation of $Sr_3Ru_2O_7$ to the Ru(V) phase $Sr_3Ru_2O_7F_2$ under one atmosphere of oxygen reveals the powerful oxidizing power of low-temperature fluorination reactions. This is further exemplified by the analogous reactions of $Sr_3(Ti_{0.5}Ru_{0.5})_2O_7$ and $Sr_3(Mn_{0.5}Ru_{0.5})_2O_7$ which are transformed into the Ru(VI) phases $Sr_3(Ti_{0.5}Ru_{0.5})_2O_7F_2$ and

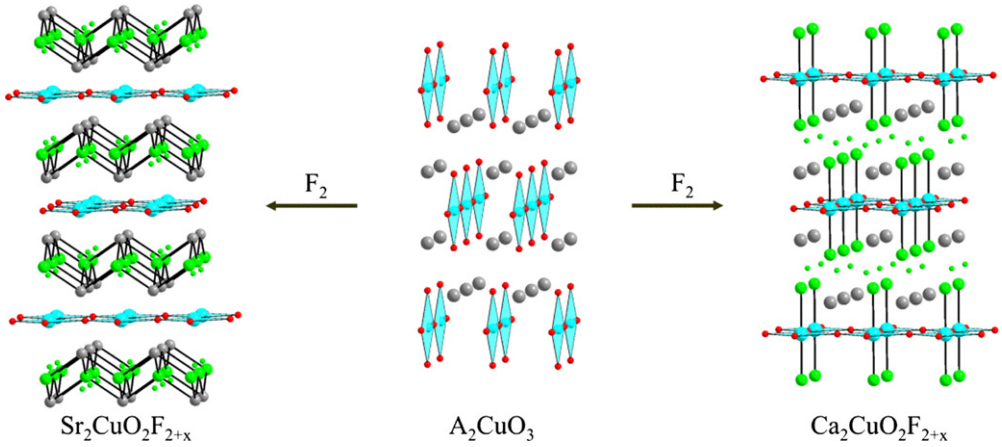

Figure 7. Fluorination of A_2CuO_3 (A = Ca, Sr) occurs with a simultaneous rearrangement of the anion lattice to retain sheets of apex-linked CuO_4 square planes.

$Sr_3(Mn_{0.5}Ru_{0.5})_2O_7F_2$, respectively, on reaction with CuF_2 under flowing oxygen [48]. By comparison the stabilization of Ru(VI) phases generally requires high oxygen pressure, for example the preparation of $Sr_2Ru_3O_{10}$ requires 0.2 GPa pressure [49].

The fluorination reactions of Ruddlesden–Popper phases do not always proceed via simple topochemical oxidative anion insertion. There can often be a degree of anion exchange involved. Thus, for example the reaction of $Sr_3(Fe_{0.5}Ru_{0.5})_2O_7$ with CuF_2/O_2 results in $Sr_3(Fe_{0.5}Ru_{0.5})_2O_{5.5}F_{3.5}$ not $Sr_3(Fe_{0.5}Ru_{0.5})_2O_7F_2$ [48]. Mössbauer spectra reveal iron retains an Fe(III) oxidation state in the fluorinated product and thus ruthenium adopts a mixed valent Ru(V/VI) combination, forcing a degree of anion exchange to occur if an $Sr_3(Fe_{0.5}Ru_{0.5})_2x_9$ (X = O, F) stoichiometry is to be adopted.

Low-temperature topochemical fluorination reactions have also been used extensively to tune the electronic behaviour of complex copper oxide phases to induce superconductivity [46]. The structural selectivity of the anion insertion/substitution reactions of these phases appears to be directed by a strong energetic preference for the preservation of CuO_4 square planar motifs. For example the fluorination of Sr_2CuO_3 to form $Sr_2CuO_2F_{2+x}$ via a combination of anion insertion and anion exchange, leads to a large-scale rearrangement of the anion lattice of the host phase. As a result the majority of the fluoride ions within the product phase are located in axial coordination sites with a small minority located within interlayer interstitial sites (figure 7) [46, 50, 51]. As a result, the SrO–SrO–CuO–SrO–SrO– stacking of the host phase is converted into SrF–F_x–SrF–CuO_2–SrF–F_x–SrF– in the product. While it is challenging to determine the oxygen-fluorine distribution in a mixed oxyfluoride by diffraction due to the similarity of both the x-ray and neutron scattering lengths of the two anions, Madelung energy calculations provide strong support for the structure shown in figure 7. The observed large-scale reorganization of the anion lattice also clearly demonstrates all the anions in the system are highly mobile.

Fluorination of the analogous calcium phase, Ca_2CuO_3, leads to a subtly different structure [52]. Reaction of Ca_2CuO_3 with fluorine gas yields $Ca_2CuO_2F_{2+x}$ in which the majority of the inserted fluoride ions now reside within interlayer interstitial sites with a small minority of fluoride ions located in sites which bond axially to the copper centres (figure 7). The structure of $Ca_2CuO_2F_{2+x}$ is therefore more closely related to the T' structure of Nd_2CuO_4 than that of the parent Ruddlesden–Popper phase. The different distribution of fluoride ions over the two coordination sites in $A_2Cu_2O_2F_{2+x}$ to yield a Ruddlesden–Popper phase when A = Sr and a T' phase when A = Ca is consistent with the small size of Ca^{2+} stabilizing the T' structure.

Summary

In conclusion it can be seen that the low-temperature topochemical manipulation of complex oxides, either by reductive anion deintercalation or oxidative anion insertion, offers many opportunities for the rational synthesis of a wide range of novel, metastable materials. As new low-temperature reactions and reagents are developed to bring about a larger variety topochemical transformations, these opportunities can only increase, offering the prospect of being able to synthesize desired solid phases on demand.

References

[1] Ruddlesden S N and Popper P 1958 *Acta Cryst.* **11** 54
[2] Schaak R E and Mallouk T E 2002 *Chem. Mater.* **14** 1455
[3] Ranmohotti K G S, Josepha E, Choi J, Zhang J X and Wiley J B 2011 *Adv. Mater.* **23** 442
[4] Hayward M A 2013 *Comprehensive Inorganic Chemistry II* 2nd edn ed J Reedijk and K R Poeppelmeier (Amsterdam: Elsevier) p 417
[5] Yamamoto T and Kageyama H 2013 *Chem. Lett.* **42** 946
[6] Gillie L J, Wright A J, Hadermann J, Van Tendeloo G and Greaves C 2003 *J. Solid State Chem.* **175** 188
[7] Millburn J E and Mitchell J F 2001 *Chem. Mater.* **13** 1957
[8] Hayward M A 2006 *Chem. Mater.* **18** 321
[9] Brese N E and O'Keeffee M 1991 *Acta Crystallogr.* B **B47** 192
[10] Hayward M A 2004 *Chem. Commun.* 170
[11] O'Malley M, Lockett M A and Hayward M A 2007 *J. Solid State Chem.* **180** 2851
[12] Romero F D and Hayward M A 2012 *Inorg. Chem.* **51** 5325

[13] Seddon J, Suard E and Hayward M A 2010 *J. Am. Chem. Soc.* **132** 2802
[14] Kitchen H J, Saratovsky I and Hayward M A 2010 *Dalton Trans.* **39** 6098
[15] Poeppelmeier K R, Leonowicz M E and Longo J M 1982 *J. Solid State Chem.* **44** 89
[16] Gillie L J, Wright A J, Hadermann J, Van Tendeloo G and Greaves C 2002 *J. Solid State Chem.* **167** 145
[17] Tassel C, Seinberg L, Hayashi N, Ganesanpotti S, Ajiro Y, Kobayashi Y and Kageyama H 2013 *Inorg. Chem.* **52** 6096
[18] Denis Romero F, Gianolio D, Cibin G, Bingham P A, d'Hollander J-C, Forder S D and Hayward M A 2013 *Inorg. Chem.* **52** 10920
[19] Hayward M A and Rosseinsky M J 2000 *Chem. Mater.* **12** 2182
[20] Choisnet J, Mouron P, Crespin M, Vanaken P A and Muller W F 1994 *J. Mater. Chem.* **4** 895
[21] Poltavets V V, Lokshin K A, Dikmen S, Croft M, Egami T and Greenblatt M 2006 *J. Am. Chem. Soc.* **128** 9050
[22] Dann S E, Weller M T and Currie D B 1992 *J. Solid State Chem.* **97** 179
[23] Kageyama H *et al* 2008 *Angew. Chem.* **47** 5704
[24] Tsujimoto Y, Tassel C, Hayashi N, Watanabe T, Kageyama H, Yoshimura K, Takano M, Ceretti M, Ritter C and Paulus W 2007 *Nature* **450** 1062
[25] Hayward M A and Rosseinsky M J 2007 *Nature* **450** 960
[26] Seinberg L *et al* 2011 *Inorg. Chem.* **50** 3988
[27] Denis Romero F, Burr S J, McGrady J E, Gianolio D, Cibin G and Hayward M A 2012 *J. Am. Chem. Soc.* **135** 1838
[28] Knee C S, Field M A L and Weller M T 2004 *Solid State Sci.* **6** 443
[29] Dixon E and Hayward M A 2010 *Inorg. Chem.* **49** 9649
[30] Dixon E and Hayward M A 2011 *Inorg. Chem.* **50** 7250
[31] Denis Romero F, Coyle L and Hayward M A 2012 *J. Am. Chem. Soc.* **134** 15946
[32] Girgsdies F and Schollhorn R 1994 *Solid State Commun.* **91** 111
[33] Jorgensen J D, Dabrowski B, Pei S, Richards D R and Hinks D G 1989 *Phys. Rev.* B **40** 2187
[34] Jorgensen J D, Dabrowski B, Pei S Y, Hinks D G, Soderholm L, Morosin B, Schirber J E, Venturini E L and Ginley D S 1988 *Phys. Rev.* B **38** 11337
[35] Nemudry A, Rudolf P and Schollhorn R 1998 *Solid State Ion.* **109** 213
[36] Dicarlo J F, Yazdi I, Bhavaraju S and Jacobson A J 1993 *Chem. Mater.* **5** 1692
[37] Amow G, Davidson I J and Skinner S J 2006 *Solid State Ion.* **177** 1205
[38] Amow G and Skinner S J 2006 *J. Solid State Electrochem.* **10** 538
[39] Bassat J M, Odier P, Villesuzanne A, Marin C and Pouchard M 2004 *Solid State Ion.* **167** 341
[40] Broux T, Prestipino C, Bahout M, Hernandez O, Swain D, Paofai S, Hansen T C and Greaves C 2013 *Chem. Mater.* **25** 4063
[41] Aikens L D, Gillie L J, Li R K and Greaves C 2002 *J. Mater. Chem.* **12** 264
[42] Sivakumar T and Wiley J B 2009 *Mater. Res. Bull.* **44** 74
[43] Aikens L D, Li R K and Greaves C 2000 *Chem. Commun.* 2129
[44] Slater P R, Hodges J P, Francesconi M G, Edwards P P, Greaves C, Gameson I and Slaski M 1995 *Physica* C **253** 16
[45] Li R K and Greaves C 2000 *Phys. Rev.* B **62** 3811
[46] Francesconi M G, Slater P R, Hodges J P, Greaves C, Edwards P P, Al-Mamouri M and Slaski M 1998 *J. Solid State Chem.* **135** 17
[47] Luo K, Tran T T, Halasyamani P S and Hayward M A 2013 *Inorg. Chem.* **52** 13762
[48] Denis Romero F, Bingham P A, Forder S D and Hayward M A 2013 *Inorg. Chem.* **52** 3388
[49] Renard C, Daviero-Minaud S and Abraham F 1999 *J. Solid State Chem.* **143** 266
[50] Almamouri M, Edwards P P, Greaves C and Slaski M 1994 *Nature* **369** 382
[51] Slater P R, Edwards P P, Greaves C, Gameson I, Francesconi M G, Hodges J P, Almamouri M and Slaski M 1995 *Physica* C **241** 151
[52] Almamouri M, Edwards P P, Greaves C, Slater P R and Slaski M 1995 *J. Mater. Chem.* **5** 913